Search for B meson decays to $\eta'\eta'K$

B. Aubert,[1] R. Barate,[1] M. Bona,[1] D. Boutigny,[1] F. Couderc,[1] Y. Karyotakis,[1] J. P. Lees,[1] V. Poireau,[1] V. Tisserand,[1] A. Zghiche,[1] E. Grauges,[2] A. Palano,[3] J. C. Chen,[4] N. D. Qi,[4] G. Rong,[4] P. Wang,[4] Y. S. Zhu,[4] G. Eigen,[5] I. Ofte,[5] B. Stugu,[5] G. S. Abrams,[6] M. Battaglia,[6] D. N. Brown,[6] J. Button-Shafer,[6] R. N. Cahn,[6] E. Charles,[6] M. S. Gill,[6] Y. Groysman,[6] R. G. Jacobsen,[6] J. A. Kadyk,[6] L. T. Kerth,[6] Yu. G. Kolomensky,[6] G. Kukartsev,[6] G. Lynch,[6] L. M. Mir,[6] P. J. Oddone,[6] T. J. Orimoto,[6] M. Pripstein,[6] N. A. Roe,[6] M. T. Ronan,[6] W. A. Wenzel,[6] M. Barrett,[7] K. E. Ford,[7] T. J. Harrison,[7] A. J. Hart,[7] C. M. Hawkes,[7] S. E. Morgan,[7] A. T. Watson,[7] K. Goetzen,[8] T. Held,[8] H. Koch,[8] B. Lewandowski,[8] M. Pelizaeus,[8] K. Peters,[8] T. Schroeder,[8] M. Steinke,[8] J. T. Boyd,[9] J. P. Burke,[9] W. N. Cottingham,[9] D. Walker,[9] T. Cuhadar-Donszelmann,[10] B. G. Fulsom,[10] C. Hearty,[10] N. S. Knecht,[10] T. S. Mattison,[10] J. A. McKenna,[10] A. Khan,[11] P. Kyberd,[11] M. Saleem,[11] L. Teodorescu,[11] V. E. Blinov,[12] A. D. Bukin,[12] V. P. Druzhinin,[12] V. B. Golubev,[12] A. P. Onuchin,[12] S. I. Serednyakov,[12] Yu. I. Skovpen,[12] E. P. Solodov,[12] K. Yu Todyshev,[12] D. S. Best,[13] M. Bondioli,[13] M. Bruinsma,[13] M. Chao,[13] S. Curry,[13] I. Eschrich,[13] D. Kirkby,[13] A. J. Lankford,[13] P. Lund,[13] M. Mandelkern,[13] R. K. Mommsen,[13] W. Roethel,[13] D. P. Stoker,[13] S. Abachi,[14] C. Buchanan,[14] S. D. Foulkes,[15] J. W. Gary,[15] O. Long,[15] B. C. Shen,[15] K. Wang,[15] L. Zhang,[15] H. K. Hadavand,[16] E. J. Hill,[16] H. P. Paar,[16] S. Rahatlou,[16] V. Sharma,[16] J. W. Berryhill,[17] C. Campagnari,[17] A. Cunha,[17] B. Dahmes,[17] T. M. Hong,[17] D. Kovalskyi,[17] J. D. Richman,[17] T. W. Beck,[18] A. M. Eisner,[18] C. J. Flacco,[18] C. A. Heusch,[18] J. Kroseberg,[18] W. S. Lockman,[18] G. Nesom,[18] T. Schalk,[18] B. A. Schumm,[18] A. Seiden,[18] P. Spradlin,[18] D. C. Williams,[18] M. G. Wilson,[18] J. Albert,[19] E. Chen,[19] A. Dvoretskii,[19] D. G. Hitlin,[19] I. Narsky,[19] T. Piatenko,[19] F. C. Porter,[19] A. Ryd,[19] A. Samuel,[19] R. Andreassen,[20] G. Mancinelli,[20] B. T. Meadows,[20] M. D. Sokoloff,[20] F. Blanc,[21] P. C. Bloom,[21] S. Chen,[21] W. T. Ford,[21] J. F. Hirschauer,[21] A. Kreisel,[21] U. Nauenberg,[21] A. Olivas,[21] W. O. Ruddick,[21] J. G. Smith,[21] K. A. Ulmer,[21] S. R. Wagner,[21] J. Zhang,[21] A. Chen,[22] E. A. Eckhart,[22] A. Soffer,[22] W. H. Toki,[22] R. J. Wilson,[22] F. Winklmeier,[22] Q. Zeng,[22] D. D. Altenburg,[23] E. Feltresi,[23] A. Hauke,[23] H. Jasper,[23] B. Spaan,[23] T. Brandt,[24] V. Klose,[24] H. M. Lacker,[24] W. F. Mader,[24] R. Nogowski,[24] A. Petzold,[24] J. Schubert,[24] K. R. Schubert,[24] R. Schwierz,[24] J. E. Sundermann,[24] A. Volk,[24] D. Bernard,[25] G. R. Bonneaud,[25] P. Grenier,[25,*] E. Latour,[25] Ch. Thiebaux,[25] M. Verderi,[25] D. J. Bard,[26] P. J. Clark,[26] W. Gradl,[26] F. Muheim,[26] S. Playfer,[26] A. I. Robertson,[26] Y. Xie,[26] M. Andreotti,[27] D. Bettoni,[27] C. Bozzi,[27] R. Calabrese,[27] G. Cibinetto,[27] E. Luppi,[27] M. Negrini,[27] A. Petrella,[27] L. Piemontese,[27] E. Prencipe,[27] F. Anulli,[28] R. Baldini-Ferroli,[28] A. Calcaterra,[28] R. de Sangro,[28] G. Finocchiaro,[28] S. Pacetti,[28] P. Patteri,[28] I. M. Peruzzi,[28,†] M. Piccolo,[28] M. Rama,[28] A. Zallo,[28] A. Buzzo,[29] R. Capra,[29] R. Contri,[29] M. Lo Vetere,[29] M. M. Macri,[29] M. R. Monge,[29] S. Passaggio,[29] C. Patrignani,[29] E. Robutti,[29] A. Santroni,[29] S. Tosi,[29] G. Brandenburg,[30] K. S. Chaisanguanthum,[30] M. Morii,[30] J. Wu,[30] R. S. Dubitzky,[31] J. Marks,[31] S. Schenk,[31] U. Uwer,[31] W. Bhimji,[32] D. A. Bowerman,[32] P. D. Dauncey,[32] U. Egede,[32] R. L. Flack,[32] J. R. Gaillard,[32] J . A. Nash,[32] M. B. Nikolich,[32] W. Panduro Vazquez,[32] X. Chai,[33] M. J. Charles,[33] U. Mallik,[33] N. T. Meyer,[33] V. Ziegler,[33] J. Cochran,[34] H. B. Crawley,[34] L. Dong,[34] V. Eyges,[34] W. T. Meyer,[34] S. Prell,[34] E. I. Rosenberg,[34] A. E. Rubin,[34] A. V. Gritsan,[35] M. Fritsch,[36] G. Schott,[36] N. Arnaud,[37] M. Davier,[37] G. Grosdidier,[37] A. Höcker,[37] F. Le Diberder,[37] V. Lepeltier,[37] A. M. Lutz,[37] A. Oyanguren,[37] S. Pruvot,[37] S. Rodier,[37] P. Roudeau,[37] M. H. Schune,[37] A. Stocchi,[37] W. F. Wang,[37] G. Wormser,[37] C. H. Cheng,[38] D. J. Lange,[38] D. M. Wright,[38] C. A. Chavez,[39] I. J. Forster,[39] J. R. Fry,[39] E. Gabathuler,[39] R. Gamet,[39] K. A. George,[39] D. E. Hutchcroft,[39] D. J. Payne,[39] K. C. Schofield,[39] C. Touramanis,[39] A. J. Bevan,[40] F. Di Lodovico,[40] W. Menges,[40] R. Sacco,[40] C. L. Brown,[41] G. Cowan,[41] H. U. Flaecher,[41] D. A. Hopkins,[41] P. S. Jackson,[41] T. R. McMahon,[41] S. Ricciardi,[41] F. Salvatore,[41] D. N. Brown,[42] C. L. Davis,[42] J. Allison,[43] N. R. Barlow,[43] R. J. Barlow,[43] Y. M. Chia,[43] C. L. Edgar,[43] M. P. Kelly,[43] G. D. Lafferty,[43] M. T. Naisbit,[43] J. C. Williams,[43] J. I. Yi,[43] C. Chen,[44] W. D. Hulsbergen,[44] A. Jawahery,[44] C. K. Lae,[44] D. A. Roberts,[44] G. Simi,[44] G. Blaylock,[45] C. Dallapiccola,[45] S. S. Hertzbach,[45] X. Li,[45] T. B. Moore,[45] S. Saremi,[45] H. Staengle,[45] S. Y. Willocq,[45] R. Cowan,[46] K. Koeneke,[46] G. Sciolla,[46] S. J. Sekula,[46] M. Spitznagel,[46] F. Taylor,[46] R. K. Yamamoto,[46] H. Kim,[47] P. M. Patel,[47] S. H. Robertson,[47] A. Lazzaro,[48] V. Lombardo,[48] F. Palombo,[48] R. Pellegrini,[48] J. M. Bauer,[49] L. Cremaldi,[49] V. Eschenburg,[49] R. Godang,[49] R. Kroeger,[49] J. Reidy,[49] D. A. Sanders,[49] D. J. Summers,[49] H. W. Zhao,[49] S. Brunet,[50] D. Côté,[50] P. Taras,[50] F. B. Viaud,[50] H. Nicholson,[51] N. Cavallo,[52,‡] G. De Nardo,[52] D. del Re,[52] F. Fabozzi,[52,‡] C. Gatto,[52] L. Lista,[52] D. Monorchio,[52] P. Paolucci,[52] D. Piccolo,[52] C. Sciacca,[52] M. Baak,[53] H. Bulten,[53] G. Raven,[53] H. L. Snoek,[53] C. P. Jessop,[54] J. M. LoSecco,[54] T. Allmendinger,[55] G. Benelli,[55] K. K. Gan,[55] K. Honscheid,[55] D. Hufnagel,[55] P. D. Jackson,[55] H. Kagan,[55] R. Kass,[55] T. Pulliam,[55] A. M. Rahimi,[55] R. Ter-Antonyan,[55] Q. K. Wong,[55] N. L. Blount,[56] J. Brau,[56] R. Frey,[56] O. Igonkina,[56] M. Lu,[56] C. T. Potter,[56] R. Rahmat,[56] N. B. Sinev,[56] D. Strom,[56] J. Strube,[56] E. Torrence,[56] F. Galeazzi,[57] A. Gaz,[57] M. Margoni,[57] M. Morandin,[57] A. Pompili,[57] M. Posocco,[57] M. Rotondo,[57]

031105-1

F. Simonetto,[57] R. Stroili,[57] C. Voci,[57] M. Benayoun,[58] J. Chauveau,[58] P. David,[58] L. Del Buono,[58] Ch. de la Vaissière,[58]
O. Hamon,[58] B. L. Hartfiel,[58] M. J. J. John,[58] J. Malclès,[58] J. Ocariz,[58] L. Roos,[58] G. Therin,[58] P. K. Behera,[59] L. Gladney,[59]
J. Panetta,[59] M. Biasini,[60] R. Covarelli,[60] M. Pioppi,[60] C. Angelini,[61] G. Batignani,[61] S. Bettarini,[61] F. Bucci,[61]
G. Calderini,[61] M. Carpinelli,[61] R. Cenci,[61] F. Forti,[61] M. A. Giorgi,[61] A. Lusiani,[61] G. Marchiori,[61] M. A. Mazur,[61]
M. Morganti,[61] N. Neri,[61] G. Rizzo,[61] J. Walsh,[61] M. Haire,[62] D. Judd,[62] D. E. Wagoner,[62] J. Biesiada,[63] N. Danielson,[63]
P. Elmer,[63] Y. P. Lau,[63] C. Lu,[63] J. Olsen,[63] A. J. S. Smith,[63] A. V. Telnov,[63] F. Bellini,[64] G. Cavoto,[64] A. D'Orazio,[64]
E. Di Marco,[64] R. Faccini,[64] F. Ferrarotto,[64] F. Ferroni,[64] M. Gaspero,[64] L. Li Gioi,[64] M. A. Mazzoni,[64] S. Morganti,[64]
G. Piredda,[64] F. Polci,[64] F. Safai Tehrani,[64] C. Voena,[64] M. Ebert,[65] H. Schröder,[65] R. Waldi,[65] T. Adye,[66] N. De Groot,[66]
B. Franek,[66] E. O. Olaiya,[66] F. F. Wilson,[66] S. Emery,[67] A. Gaidot,[67] S. F. Ganzhur,[67] G. Hamel de Monchenault,[67]
W. Kozanecki,[67] M. Legendre,[67] G. Vasseur,[67] Ch. Yèche,[67] M. Zito,[67] W. Park,[68] M. V. Purohit,[68] J. R. Wilson,[68]
M. T. Allen,[69] D. Aston,[69] R. Bartoldus,[69] P. Bechtle,[69] N. Berger,[69] A. M. Boyarski,[69] R. Claus,[69] J. P. Coleman,[69]
M. R. Convery,[69] M. Cristinziani,[69] J. C. Dingfelder,[69] D. Dong,[69] J. Dorfan,[69] G. P. Dubois-Felsmann,[69] D. Dujmic,[69]
W. Dunwoodie,[69] R. C. Field,[69] T. Glanzman,[69] S. J. Gowdy,[69] M. T. Graham,[69] V. Halyo,[69] C. Hast,[69] T. Hryn'ova,[69]
W. R. Innes,[69] M. H. Kelsey,[69] P. Kim,[69] M. L. Kocian,[69] D. W. G. S. Leith,[69] S. Li,[69] J. Libby,[69] S. Luitz,[69] V. Luth,[69]
H. L. Lynch,[69] D. B. MacFarlane,[69] H. Marsiske,[69] R. Messner,[69] D. R. Muller,[69] C. P. O'Grady,[69] V. E. Ozcan,[69] M. Perl,[69]
A. Perazzo,[69] B. N. Ratcliff,[69] A. Roodman,[69] A. A. Salnikov,[69] R. H. Schindler,[69] J. Schwiening,[69] A. Snyder,[69]
J. Stelzer,[69] D. Su,[69] M. K. Sullivan,[69] K. Suzuki,[69] S. K. Swain,[69] J. M. Thompson,[69] J. Va'vra,[69] N. van Bakel,[69]
M. Weaver,[69] A. J. R. Weinstein,[69] W. J. Wisniewski,[69] M. Wittgen,[69] D. H. Wright,[69] A. K. Yarritu,[69] K. Yi,[69]
C. C. Young,[69] P. R. Burchat,[70] A. J. Edwards,[70] S. A. Majewski,[70] B. A. Petersen,[70] C. Roat,[70] L. Wilden,[70] S. Ahmed,[71]
M. S. Alam,[71] R. Bula,[71] J. A. Ernst,[71] V. Jain,[71] B. Pan,[71] M. A. Saeed,[71] F. R. Wappler,[71] S. B. Zain,[71] W. Bugg,[72]
M. Krishnamurthy,[72] S. M. Spanier,[72] R. Eckmann,[73] J. L. Ritchie,[73] A. Satpathy,[73] C. J. Schilling,[73] R. F. Schwitters,[73]
J. M. Izen,[74] I. Kitayama,[74] X. C. Lou,[74] S. Ye,[74] F. Bianchi,[75] F. Gallo,[75] D. Gamba,[75] M. Bomben,[76] L. Bosisio,[76]
C. Cartaro,[76] F. Cossutti,[76] G. Della Ricca,[76] S. Dittongo,[76] S. Grancagnolo,[76] L. Lanceri,[76] L. Vitale,[76] V. Azzolini,[77]
F. Martinez-Vidal,[77] Sw. Banerjee,[78] B. Bhuyan,[78] C. M. Brown,[78] D. Fortin,[78] K. Hamano,[78] R. Kowalewski,[78]
I. M. Nugent,[78] J. M. Roney,[78] R. J. Sobie,[78] J. J. Back,[79] P. F. Harrison,[79] T. E. Latham,[79] G. B. Mohanty,[79]
M. Pappagallo,[79] H. R. Band,[80] X. Chen,[80] B. Cheng,[80] S. Dasu,[80] M. Datta,[80] A. M. Eichenbaum,[80] K. T. Flood,[80]
J. J. Hollar,[80] P. E. Kutter,[80] H. Li,[80] R. Liu,[80] B. Mellado,[80] A. Mihalyi,[80] A. K. Mohapatra,[80] Y. Pan,[80] M. Pierini,[80]
R. Prepost,[80] P. Tan,[80] S. L. Wu,[80] Z. Yu,[80] and H. Neal[81]

(*BABAR* Collaboration)

[1]*Laboratoire de Physique des Particules, F-74941 Annecy-le-Vieux, France*
[2]*Universitat de Barcelona, Facultat de Fisica Dept. ECM, E-08028 Barcelona, Spain*
[3]*Università di Bari, Dipartimento di Fisica and INFN, I-70126 Bari, Italy*
[4]*Institute of High Energy Physics, Beijing 100039, China*
[5]*University of Bergen, Institute of Physics, N-5007 Bergen, Norway*
[6]*Lawrence Berkeley National Laboratory and University of California, Berkeley, California 94720, USA*
[7]*University of Birmingham, Birmingham, B15 2TT, United Kingdom*
[8]*Ruhr Universität Bochum, Institut für Experimentalphysik 1, D-44780 Bochum, Germany*
[9]*University of Bristol, Bristol BS8 1TL, United Kingdom*
[10]*University of British Columbia, Vancouver, British Columbia, Canada V6T 1Z1*
[11]*Brunel University, Uxbridge, Middlesex UB8 3PH, United Kingdom*
[12]*Budker Institute of Nuclear Physics, Novosibirsk 630090, Russia*
[13]*University of California at Irvine, Irvine, California 92697, USA*
[14]*University of California at Los Angeles, Los Angeles, California 90024, USA*
[15]*University of California at Riverside, Riverside, California 92521, USA*
[16]*University of California at San Diego, La Jolla, California 92093, USA*
[17]*University of California at Santa Barbara, Santa Barbara, California 93106, USA*
[18]*University of California at Santa Cruz, Institute for Particle Physics, Santa Cruz, California 95064, USA*
[19]*California Institute of Technology, Pasadena, California 91125, USA*
[20]*University of Cincinnati, Cincinnati, Ohio 45221, USA*
[21]*University of Colorado, Boulder, Colorado 80309, USA*
[22]*Colorado State University, Fort Collins, Colorado 80523, USA*
[23]*Universität Dortmund, Institut für Physik, D-44221 Dortmund, Germany*
[24]*Technische Universität Dresden, Institut für Kern- und Teilchenphysik, D-01062 Dresden, Germany*

[25]*Ecole Polytechnique, LLR, F-91128 Palaiseau, France*

[26]*University of Edinburgh, Edinburgh EH9 3JZ, United Kingdom*

[27]*Università di Ferrara, Dipartimento di Fisica and INFN, I-44100 Ferrara, Italy*

[28]*Laboratori Nazionali di Frascati dell'INFN, I-00044 Frascati, Italy*

[29]*Università di Genova, Dipartimento di Fisica and INFN, I-16146 Genova, Italy*

[30]*Harvard University, Cambridge, Massachusetts 02138, USA*

[31]*Universität Heidelberg, Physikalisches Institut, Philosophenweg 12, D-69120 Heidelberg, Germany*

[32]*Imperial College London, London, SW7 2AZ, United Kingdom*

[33]*University of Iowa, Iowa City, Iowa 52242, USA*

[34]*Iowa State University, Ames, Iowa 50011-3160, USA*

[35]*Johns Hopkins University, Baltimore, Maryland 21218, USA*

[36]*Universität Karlsruhe, Institut für Experimentelle Kernphysik, D-76021 Karlsruhe, Germany*

[37]*Laboratoire de l'Accélérateur Linéaire, IN2P3-CNRS et Université Paris-Sud 11,*
Centre Scientifique d'Orsay, B.P. 34, F-91898 ORSAY Cedex, France

[38]*Lawrence Livermore National Laboratory, Livermore, California 94550, USA*

[39]*University of Liverpool, Liverpool L69 7ZE, United Kingdom*

[40]*Queen Mary, University of London, E1 4NS, United Kingdom*

[41]*University of London, Royal Holloway and Bedford New College, Egham, Surrey TW20 0EX, United Kingdom*

[42]*University of Louisville, Louisville, Kentucky 40292, USA*

[43]*University of Manchester, Manchester M13 9PL, United Kingdom*

[44]*University of Maryland, College Park, Maryland 20742, USA*

[45]*University of Massachusetts, Amherst, Massachusetts 01003, USA*

[46]*Massachusetts Institute of Technology, Laboratory for Nuclear Science, Cambridge, Massachusetts 02139, USA*

[47]*McGill University, Montréal, Québec, Canada H3A 2T8*

[48]*Università di Milano, Dipartimento di Fisica and INFN, I-20133 Milano, Italy*

[49]*University of Mississippi, University, Mississippi 38677, USA*

[50]*Université de Montréal, Physique des Particules, Montréal, Québec, Canada H3C 3J7*

[51]*Mount Holyoke College, South Hadley, Massachusetts 01075, USA*

[52]*Università di Napoli Federico II, Dipartimento di Scienze Fisiche and INFN, I-80126, Napoli, Italy*

[53]*NIKHEF, National Institute for Nuclear Physics and High Energy Physics, NL-1009 DB Amsterdam, The Netherlands*

[54]*University of Notre Dame, Notre Dame, Indiana 46556, USA*

[55]*Ohio State University, Columbus, Ohio 43210, USA*

[56]*University of Oregon, Eugene, Oregon 97403, USA*

[57]*Università di Padova, Dipartimento di Fisica and INFN, I-35131 Padova, Italy*

[58]*Universités Paris VI et VII, Laboratoire de Physique Nucléaire et de Hautes Energies, F-75252 Paris, France*

[59]*University of Pennsylvania, Philadelphia, Pennsylvania 19104, USA*

[60]*Università di Perugia, Dipartimento di Fisica and INFN, I-06100 Perugia, Italy*

[61]*Università di Pisa, Dipartimento di Fisica, Scuola Normale Superiore and INFN, I-56127 Pisa, Italy*

[62]*Prairie View A&M University, Prairie View, Texas 77446, USA*

[63]*Princeton University, Princeton, New Jersey 08544, USA*

[64]*Università di Roma La Sapienza, Dipartimento di Fisica and INFN, I-00185 Roma, Italy*

[65]*Universität Rostock, D-18051 Rostock, Germany*

[66]*Rutherford Appleton Laboratory, Chilton, Didcot, Oxon, OX11 0QX, United Kingdom*

[67]*DSM/Dapnia, CEA/Saclay, F-91191 Gif-sur-Yvette, France*

[68]*University of South Carolina, Columbia, South Carolina 29208, USA*

[69]*Stanford Linear Accelerator Center, Stanford, California 94309, USA*

[70]*Stanford University, Stanford, California 94305-4060, USA*

[71]*State University of New York, Albany, New York 12222, USA*

[72]*University of Tennessee, Knoxville, Tennessee 37996, USA*

[73]*University of Texas at Austin, Austin, Texas 78712, USA*

[74]*University of Texas at Dallas, Richardson, Texas 75083, USA*

[75]*Università di Torino, Dipartimento di Fisica Sperimentale and INFN, I-10125 Torino, Italy*

[76]*Università di Trieste, Dipartimento di Fisica and INFN, I-34127 Trieste, Italy*

[77]*IFIC, Universitat de Valencia-CSIC, E-46071 Valencia, Spain*

[78]*University of Victoria, Victoria, British Columbia, Canada V8W 3P6*

[79]*Department of Physics, University of Warwick, Coventry CV4 7AL, United Kingdom*

---

[*]Also at Laboratoire de Physique Corpusculaire, Clermont-Ferrand, France

[†]Also with Università di Perugia, Dipartimento di Fisica, Perugia, Italy

[‡]Also with Università della Basilicata, Potenza, Italy

^{80}*University of Wisconsin, Madison, Wisconsin 53706, USA*
^{81}*Yale University, New Haven, Connecticut 06511, USA*

We describe searches for decays of B mesons to the charmless final states $\eta'\eta'K$. The data consist of 228×10^6 $B\bar{B}$ pairs produced in e^+e^- annihilation, collected with the *BABAR* detector at the Stanford Linear Accelerator Center. The 90% confidence level upper limits for the branching fractions are $\mathcal{B}(B^0 \to \eta'\eta'K^0) < 31 \times 10^{-6}$ and $\mathcal{B}(B^+ \to \eta'\eta'K^+) < 25 \times 10^{-6}$.

The phenomenon of *CP* violation has been extensively studied in recent years at the *B* factories. The observations of mixing-induced *CP* violation in $B^0 \to J/\psi K_S^0$ decays [1] and of direct *CP* violation both in the neutral kaon system [2] and in $B^0 \to K^+\pi^-$ decays [3] are in agreement with expectations in the standard model (SM) of electroweak interactions [4]. Some possible evidence of disagreement between experimental results and SM expectations is found in *B* decay modes dominated by penguin amplitudes, for example, in the decay $B^0 \to \eta'K_S^0$ [5]. Further important information about *CP* violation and hadronic *B* decays can be provided by the measurements of branching fractions and time-dependent *CP* asymmetries in *B* decays to three-body final states containing two identical neutral particles of spin zero and another spin zero neutral particle [6]. An example of such a decay is $B^0 \to K_S^0 K_S^0 K_S^0$, which has already been observed [7]. Since the branching fractions for the decays $B \to \eta'K$ are large [5], another example which might be particularly interesting for time-dependent *CP* violation analysis is the mode $B^0 \to \eta'\eta'K^0$.

We present the results of searches for the exclusive decay modes $B^+ \to \eta'\eta'K^+$ [8] and $B^0 \to \eta'\eta'K^0$, which are studied for the first time. The results are based on data collected with the *BABAR* detector [9] at the PEP-II asymmetric-energy e^+e^- collider [10] located at the Stanford Linear Accelerator Center. The analyses use an integrated luminosity of 207 fb^{-1}, corresponding to 228×10^6 $B\bar{B}$ pairs, recorded at the $\Upsilon(4S)$ resonance (center-of-mass energy $\sqrt{s} = 10.58$ GeV).

Charged particles from the e^+e^- interactions are detected, and their momenta measured, by a combination of five layers of double-sided silicon microstrip detectors and a 40-layer drift chamber, both operating in the 1.5 -T magnetic field of a superconducting solenoid. Photons and electrons are identified with a CsI(Tl) crystal electromagnetic calorimeter (EMC), covering 90% of the 4π in the $\Upsilon(4S)$ rest frame. The energy resolution σ_E/E is 3% [9]. Further charged particle identification (PID) is provided by the average energy loss (dE/dx) in the tracking devices and by an internally reflecting, ring-imaging Cherenkov detector (DIRC) covering the central region. A K/π separation of better than 4 standard deviations (σ) is achieved for momenta below 3 GeV/c, decreasing to 2.5σ at the highest momenta in the *B* decay final states.

The *B* daughter candidates are reconstructed through their decays $\eta' \to \eta\pi^+\pi^-$ ($\eta'_{\eta\pi\pi}$), where $\eta \to \gamma\gamma$, and $\eta' \to \rho^0\gamma$ ($\eta'_{\rho\gamma}$), where $\rho^0 \to \pi^+\pi^-$. We require the laboratory energy of the photons to be greater than 30 MeV for $\eta'_{\eta\pi\pi}$ and 200 Me V for $\eta'_{\rho\gamma}$. We impose the following requirements on the invariant mass (in MeV/c^2) of the candidate final states: $490 < m(\gamma\gamma) < 600$ for η, $930 < m(\pi^+\pi^-\eta) < 990$ for $\eta'_{\eta\pi\pi}$, $930 < m(\pi^+\pi^-\gamma) < 990$ for $\eta'_{\rho\gamma}$, and $510 < m(\pi^+\pi^-) < 1000$ for ρ^0. Secondary tracks in η' candidates are rejected if their PID signatures from the DIRC and dE/dx are consistent with those for protons, kaons, or electrons. Charged K candidates are selected if their PID signatures from the DIRC and dE/dx are consistent with that for kaons. Candidate K_S^0 decays are formed from pairs of oppositely charged tracks with $486 < m(\pi^+\pi^-) < 510$ MeV/c^2, a decay vertex χ^2 probability larger than 0.001, and a reconstructed decay length greater than 3 times its uncertainty.

We reconstruct the *B* meson candidate by combining two η' candidates and a charged or neutral kaon. We consider only cases with two $\eta'_{\eta\pi\pi}$ candidates or a $\eta'_{\eta\pi\pi}$ and a $\eta'_{\rho\gamma}$. We do not consider the case with two $\eta'_{\rho\gamma}$ candidates due to the high background present in this mode. From the kinematics of the $\Upsilon(4S)$ decays we determine the energy-substituted mass $m_{ES} = \sqrt{\frac{1}{4}s - \mathbf{p}_B^2}$ and the energy difference $\Delta E = E_B - \frac{1}{2}\sqrt{s}$, where $(E_B, \mathbf{p}_B)$ is the *B* meson 4-momentum vector, and all values are expressed in the $\Upsilon(4S)$ frame. The resolution is 3.0 MeV/c^2 for m_{ES} and 26 MeV for ΔE. We require 5.25 GeV/$c^2 < m_{ES} < 5.29$ GeV/c^2 and $|\Delta E| < 0.2$ GeV.

Backgrounds arise primarily from random combinations of particles in continuum $e^+e^- \to q\bar{q}$ events ($q = u, d, s, c$). We reduce these with requirements on the angle θ_T between the thrust axis of the *B* candidate in the $\Upsilon(4S)$ frame and that of the rest of the charged tracks and neutral calorimeter clusters in the event. The distribution is sharply peaked near $|\cos\theta_T| = 1$ for $q\bar{q}$ jet pairs, and nearly uniform for *B* meson decays. The requirement is $|\cos\theta_T| < 0.9$ ($|\cos\theta_T| < 0.7$ for the charged mode with $\eta'_{\rho\gamma}$). For the ρ decays we also use $\mathcal{H} \equiv |\cos\theta^\rho|$ where the helicity angle θ^ρ is defined as the angle between the momenta of a daughter particle and the η', measured in the ρ meson rest frame. We require for the $\eta'_{\rho\gamma}$ decay $\mathcal{H} < 0.9$. Events

are retained only if they contain one or more charged tracks that are not used in the candidate decay.

We obtain the signal event yields from unbinned extended maximum likelihood fits. The input observables are ΔE, m_{ES}, the invariant masses of the two η' ($m_{\eta'1}$, $m_{\eta'2}$), a Fisher discriminant $\mathcal{F}$ [11], and the variable $\mathcal{H}$ in the decay modes containing the ρ meson in final state. The Fisher discriminant $\mathcal{F}$ is a linear combination of four event shape variables: the angles, with respect to the beam axis, of the *B* momentum and the *B* thrust axis (in the $\Upsilon(4S)$ frame), and the zeroth and second angular moments $L_{0,2}$ of the energy flow about the *B* thrust axis [12]. The moments are defined by $L_j = \sum_i p_i \times |\cos\theta_i|^j$, where θ_i is the angle, with respect to the *B* thrust axis, of track or neutral cluster *i*, and p_i is its momentum. The sum excludes the *B* candidate daughters. The coefficients used in the combination of these variables are chosen to maximize the separation between the signal and the continuum background, and are determined from studies of signal MC and m_{ES} and ΔE sideband data ($5.25 < m_{ES} < 5.27$ GeV/c^2, $0.1 < |\Delta E| < 0.2$ GeV).

The average number of candidates found per selected event is in the range 1.5 to 1.8, depending on the final state. We choose the candidate with the highest *B* vertex χ^2 probability. From simulated events we find that this algorithm selects the correct candidate in about 82% of the events containing multiple candidates, and introduces negligible bias.

We use Monte Carlo (MC) simulation to estimate backgrounds from other *B* decays, including final states with and without charm. These contributions are negligible for the $\eta'_{\eta\pi\pi}$ modes. For $\eta'_{\rho\gamma}$ we include a $B\bar{B}$ component in the fit. We consider four categories in the likelihood fit: signal, self-cross feed (SCF) signal, defined as a signal candidate where one *B* candidate daughter has been exchanged with a particle from the rest of the event, and continuum and $B\bar{B}$ backgrounds.

For each event *i* and category *j*, we define the probability density function (PDF)

$$\mathcal{P}^i_j = \mathcal{P}_j(m^i_{ES})\mathcal{P}_j(\Delta E^i)\mathcal{P}_j(\mathcal{F}^i)\mathcal{P}_j(m^i_{\eta'1})$$
$$\times \mathcal{P}_j(m^i_{\eta'2})\mathcal{P}_j(\mathcal{H}^i) \qquad (1)$$

The likelihood function is

$$L = e^{-(\sum n_j)}\prod_{i=1}^{N}\left[\sum_{j=1}^{4} n_j \mathcal{P}^i_j\right], \qquad (2)$$

where *N* is the number of candidates, n_j is the number of events in category *j* which is returned by the fit, and $\mathcal{P}^i_j$ is the corresponding PDF, evaluated with the observables of the *i*th event. Since correlations among the observables are small, we take each $\mathcal{P}$ as the product of the PDFs for the separate variables. We determine the PDF parameters from Monte Carlo simulation [13] of the signal, SCF, and $B\bar{B}$

background, while using m_{ES} and ΔE sideband data to model the PDFs of continuum background.

We parameterize each of the functions $\mathcal{P}(m_{ES})$, $\mathcal{P}(\Delta E)$, $\mathcal{P}(m_{\eta'})$, and $\mathcal{P}(m_\eta)$ for signal and SCF with two Gaussian distributions. The m_{ES} distribution for $B\bar{B}$ and continuum background is described by a threshold function [14]. The ΔE distribution for $B\bar{B}$ and continuum background and the $\mathcal{H}$ distributions are represented by linear or quadratic functions. The distributions of $m_{\eta'}$ and m_η in $B\bar{B}$ and continuum background are described by a Gaussian plus linear function. The distribution of $\mathcal{F}$ is described with an asymmetric Gaussian function with a different width below and above the peak. We allow the continuum background PDF parameters to vary in the fit. Large control samples of $B \rightarrow D(K\pi\pi)\pi$ decays are used to verify the simulated ΔE and m_{ES} resolution. Any bias in the fit, which arises mainly from neglecting the small correlations among the discriminating variables, is determined from a large set of simulated experiments in which the $q\bar{q}$ background is generated from the PDFs, and into which we have embedded the expected number of $B\bar{B}$ background and signal events chosen randomly from fully simulated Monte Carlo samples.

In Table I we show the fitted signal yield, the fit bias in events, the detection efficiency, the product of daughter branching fractions for each decay mode, the significance $\mathcal{S}$ (σ), and the measured branching fraction. We compute the branching fractions from the fitted signal event yields, detection efficiencies, daughter branching fractions, and number of produced *B* mesons, assuming equal production rates of charged and neutral *B* meson pairs. We correct the yield for the fit bias estimated with the simulations. We combine results from different subdecay modes by adding the values of $-2\ln L$, taking proper account of the correlated and uncorrelated systematic uncertainties. We report the statistical significance and branching fraction for the individual decay channels. For the combined measurements we also report the 90% confidence level (CL) upper limit. The statistical error on the signal yield is the change in the central value when the quantity $-2\ln L$ increases by one unit from its minimum value. The significance is the square root of the difference between the value of $-2\ln L$ (with systematic uncertainties included) for zero signal and the value at its minimum. The 90% CL upper limit is taken to be the branching fraction below which lies 90% of the total likelihood integral in the positive branching fraction region.

Figure 1 shows projections of charged and neutral $\eta'\eta'K$ candidates onto m_{ES} and ΔE for the subset of candidates for which the signal likelihood (computed without the variable plotted) exceeds a mode-dependent threshold that optimizes the sensitivity.

In Fig. 2 we show the distribution of the ratio between the likelihood L(Sg) for the signal category and the sum of the likelihoods for signal and all background categories

TABLE I.   Fitted signal yield, fit bias, detection efficiency ϵ, daughter branching fraction product $\prod \mathcal{B}_i$, significance $\mathcal{S}$, measured branching fraction $\mathcal{B}$ with statistical error for each decay mode. For the combined measurements we give the significance (with systematic uncertainties included) and the branching fraction with statistical and systematic uncertainty (in parentheses the 90% CL upper limit).

Mode	Yield	Fit bias (ev)	ϵ (%)	$\prod \mathcal{B}_i$ (%)	$\mathcal{S}$ (σ)	$\mathcal{B}(10^{-6})$
$\eta'_{\eta\pi\pi}\eta'_{\eta\pi\pi}K^0$	$0.9^{+1.4}_{-0.7}$	$+0.5$	2.9	1.1	0.5	6^{+20}_{-10}
$\eta'_{\eta\pi\pi}\eta'_{\rho\gamma}K^0$	$4.1^{+8.1}_{-6.7}$	$+3.8$	3.7	3.6	0.0	1^{+27}_{-22}
$\boldsymbol{\eta'\eta'K^0}$					**0.5**	$\boldsymbol{5^{+14}_{-9} \pm 1(<31)}$
$\eta'_{\eta\pi\pi}\eta'_{\eta\pi\pi}K^+$	$4.2^{+3.7}_{-2.8}$	$+0.5$	3.5	3.1	2.1	15^{+15}_{-11}
$\eta'_{\eta\pi\pi}\eta'_{\rho\gamma}K^+$	$13.6^{+11.7}_{-10.1}$	$+8.5$	3.4	10.4	0.5	6^{+15}_{-13}
$\boldsymbol{\eta'\eta'K^+}$					**2.0**	$\boldsymbol{11^{+9}_{-7} \pm 1(<25)}$

L(Bg) for data and for simulation generated from the PDF model. We see good agreement between the model and the data. By construction the background is concentrated near zero, while any signal would appear as an excess of events near one.

The main sources of systematic errors include uncertainties in the PDF parameters and the maximum likelihood fit bias. For the signal, the uncertainties in the PDF parameters are estimated by comparing MC and data in control samples. Varying the signal PDF parameters within these uncertainties, we estimate yield uncertainties up to 1 event, depending on the mode. The uncertainty from the fit bias is taken as half the correction itself (up to 4 events). Uncertainties in our knowledge of the efficiency, found from auxiliary studies, include $0.8\% \times N_t$ and $1.5\% \times N_\gamma$, where N_t and N_γ are the numbers of tracks and photons, respectively, in the B candidate. A systematic uncertainty of 1.8% is assigned to single photon reconstruction efficiency. There is a systematic error of 2.1% in the efficiency of K_S^0 reconstruction and 3.0% per η in the efficiency of η

reconstruction. The uncertainty in the total number of $B\bar{B}$ pairs in the data sample is 1.1%. Published data [15] provide the uncertainties in the B daughter product branching fractions (3.5–4.9%).

In conclusion, we have measured 90% CL upper limits for the branching fractions: $\mathcal{B}(B^0 \to \eta'\eta'K^0) < 31 \times 10^{-6}$ and $\mathcal{B}(B^+ \to \eta'\eta'K^+) < 25 \times 10^{-6}$. From these results we conclude that no CP study is feasible in these B decays with the currently available data samples.

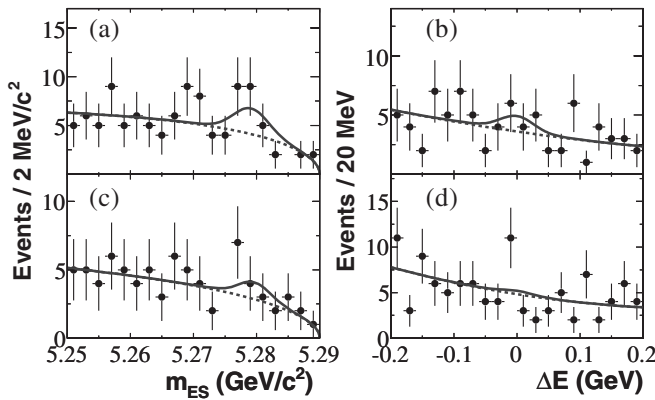FIG. 1.   The B candidate m_{ES} and ΔE projections for $\eta'\eta'K^+$ (a), (b) and $\eta'\eta'K_S^0$ (c), (d) for the combined subdecay modes. Points with errors represent the data, solid curves the full fit functions and dashed curves the background functions. These plots are made with a requirement on the likelihood and thus do not show all events in the data samples.
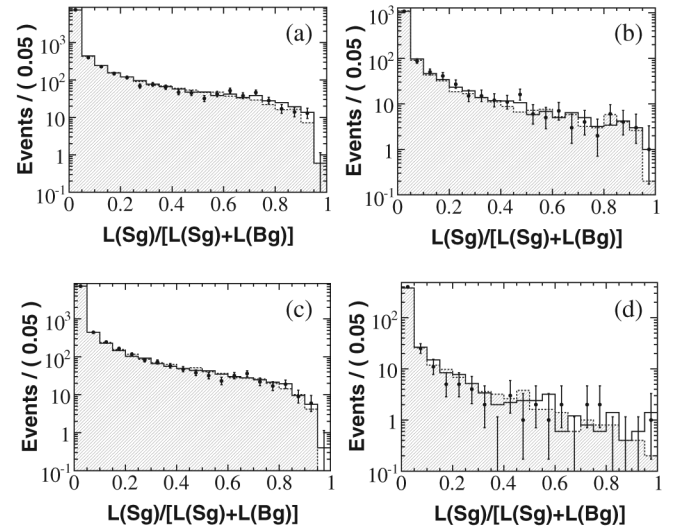

FIG. 2.   The likelihood ratio L(Sg)/[L(Sg)+ L(Bg)] for the subdecay modes of $\eta'\eta'K$: (a) $\eta'_{\eta\pi\pi}\eta'_{\rho\gamma}K^+$, (b) $\eta'_{\eta\pi\pi}\eta'_{\eta\pi\pi}K^+$, (c) $\eta'_{\eta\pi\pi}\eta'_{\rho\gamma}K_S^0$, (d) $\eta'_{\eta\pi\pi}\eta'_{\eta\pi\pi}K_S^0$. The on-resonance data are shown as points with error bars; the sum of all simulated background samples is shown by the shaded (dashed line) histograms; and the sum of these backgrounds plus the signal from the PDF model are given by the open (solid line) histograms.

[1] B. Aubert *et al.* (*BABAR* Collaboration), Phys. Rev. Lett. **87**, 091801 (2001); B. Aubert *et al.* (*BABAR* Collaboration), Phys. Rev. Lett. **89**, 201802 (2002); K. Abe *et al.* (Belle Collaboration), Phys. Rev. Lett. **93**, 191802 (2004); K. Abe *et al.* (Belle Collaboration), Phys. Rev. D **66**, 071102 (2002).

[2] J. R. Batley *et al.* (NA48 Collaboration), Phys. Lett. B **544**, 97 (2002); A. Alavi-Harati *et al.* (KTeV Collaboration), Phys. Rev. D **67**, 012005 (2003).

[3] B. Aubert *et al.* (*BABAR* Collaboration), Phys. Rev. Lett. **93**, 131801 (2004); K. Abe *et al.* (Belle Collaboration), Phys. Rev. Lett. **93**, 191802 (2004).

[4] N. Cabibbo, Phys. Rev. Lett. **10**, 531 (1963); M. Kobayashi and T. Maskawa, Prog. Theor. Phys. **49**, 652 (1973).

[5] B. Aubert *et al.* (*BABAR* Collaboration), Phys. Rev. Lett. **91**, 161801 (2003).

[6] T. Gershon and M. Hazumi, Phys. Lett. B **596**, 163 (2004).

[7] A. Garmash *et al.* (Belle Collaboration), Phys. Rev. D **69**, 012001 (2004); B. Aubert *et al.* (*BABAR* Collaboration), Phys. Rev. Lett. **95**, 011801 (2005).

[8] Charge-conjugate modes are implied throughout.

[9] B. Aubert *et al.* (*BABAR* Collaboration), Nucl. Instr. Methods Phys. Res., Sect. A **479**, 1 (2002).

[10] PEP-II, Conceptual Design Report, Report No. SLAC-R-418, 1993 (unpublished).

[11] R. A. Fisher, Annals of Eugenics **7**, 179 (1936).

[12] B. Aubert *et al.* (*BABAR* Collaboration), Phys. Rev. D **70**, 032006 (2004).

[13] The BaBar detector Monte Carlo simulation is based on GEANT4: S. Agostinelli *et al.*, Nucl. Instr. Methods Phys. Res., Sect. A **506**, 250 (2003).

[14] The threshold function is defined as $x\sqrt{1-x^2}\exp[-\xi(1-x^2)]$, with $x \equiv 2m_{ES}/\sqrt{s}$ and ξ is a parameter that is determined by the fit: H. Albrecht *et al.* (ARGUS Collaboration), Phys. Lett. B **241**, 278 (1990).

[15] S. Eidelman *et al.* (Particle Data Group), Phys. Lett. B **592**, 1 (2004).